

Λ polarization from thermalized jet energy

Willian Matioli Serenone^{a,*}, João Guilherme Prado Barbon^a, David Dobrigkeit Chinellato^a, Michael Annan Lisa^b, Chun Shen^{c,d}, Jun Takahashi^a, Giorgio Torrieri^a

^a*Instituto de Física Gleb Wataghin, Universidade Estadual de Campinas, Campinas, Brasil*

^b*The Ohio State University, Columbus, Ohio, USA*

^c*Department of Physics and Astronomy, Wayne State University, Detroit, MI 48201, USA*

^d*RIKEN BNL Research Center, Brookhaven National Laboratory Upton, NY 11973, USA*

Abstract

We examine the formation of vortical “smoke rings” as a result of thermalization of energy lost by a jet. We simulate the formation and evolution of these rings using hydrodynamics and define an observable that allows to probe this phenomenon experimentally. We argue that observation of vorticity associated with jets would be an experimental confirmation of the thermalization of the energy lost by quenched jets, and also a probe of shear viscosity.

1. Introduction

Two of the most studied results in heavy ion physics at ultra-relativistic energies are jet energy loss [1, 2, 3, 4, 5] and fluid behavior [6, 7, 8, 9, 10, 11]. The first shows that colored degrees of freedom form “a medium” opaque to fast partons, and the second shows this medium thermalizes very quickly and subsequent evolution is nearly inviscid. Both results are usually interpreted as evidence that the medium created in heavy ion collisions is a “strongly coupled liquid”.

However, considerable theoretical uncertainty exists regarding the fate of the energy lost by the jet. If the plasma is a very good fluid it is a reasonable hypothesis that the jet energy should thermalize and contribute to the fluid flow gradients. However, we do not have a clear experimental signature of this. Partially, this is because the models of parton-medium interaction are inconclusive [12], and partially it is because direct signatures of fluid behavior, such as “Conical flow”, have not been conclusively observed [13, 14].

Recently, a new intriguing manifestation of hydrodynamic behavior has been found: Λ polarization, measurable via parity violating decays [15]. It seems to be aligned to the global vorticity of the fluid and, to an extent, with near-ideal hydrodynamic vorticity being transferred into Polarization via an isentropic transition, respecting angular momentum conservation [16]. As well as a further confirmation of the fluid-like behav-

ior of the medium, this observation opens the door to use polarization as a tool to study the medium’s dynamics.

We propose to use polarization to understand the fate of locally thermalized energy emitted by the jet. A schematic picture of the physical situation is shown in Fig. 1. A hard parton generates a dijet structure and one of these is partially quenched by the quark-gluon plasma, while the other is not. The quenched portion of the jet introduces a initial velocity gradient in the fluid. As is known from everyday physics, smoke-rings, eddies and so on are ubiquitous in fluids when a velocity gradient is present. This is certainly the case when a fast parton deposits energy into a medium. The only difficulty is, of course, that the jet’s direction fluctuates event-by-event which vanishes after the event averaging.

This is, however, easily surmountable: As argued in [17], the interplay between vorticity and transverse expansion can be used to define a “jet production plane”. This insight can be sharpened into the definition of an experimental observable that ties the polarization direction, the angular momentum and a desired reference vector, which can be defined event-by-event. In this work, we shall focus on defining the reference vector as a high- p_T trigger particle. This observable, if measured to be non-zero in classes of events where jet suppression exists, would provide unique and compelling evidence that the energy lost by the jet is indeed thermalized. Moreover, it can be used to infer the medium’s viscosity, provided the initial velocity gradients generated by the jet are quantified.

*Corresponding author

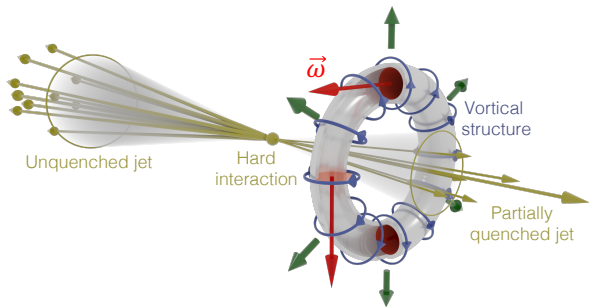


Figure 1: Schematic representation of the physical situation proposed. A hard parton generates a dijet structure and one of these jets is partially quenched by the quark-gluon plasma, while the other is not. The quenched portion of the jet introduces a momentum gradient in the fluid which in turn will generate a vortex ring.

2. A model for the jet thermalization

Our first step is to choose a suitable model for the medium in which the jet will deposit (part of) its energy. We choose a model which incorporates three dimensional features, since the Λ polarization calculation we will perform later on will depend on the dynamics in all dimensions. The need to perform (3+1)D simulation imposes a heavy computational constraint. To make our work feasible, we take the average over a thousand initial conditions, generated with T_RENTo 3D [18] configured for simulations of Pb–Pb collisions at $\sqrt{s_{NN}} = 2.76$ TeV, all of them with impact parameter $b = 0$ fm. The other parameters used to generate these initial conditions were obtained from Ref. [19] (for parameters common to 2D and 3D T_RENTo) and Ref. [18] (for parameters exclusive to 3D T_RENTo). These are summarized in Table 1. All computations are made in a grid with spacing equal to 0.1 fm in the x and y directions¹ and 0.2 in the spatial rapidity (η_s) direction.

We expect the event-averaged fluid background to give a good estimation on the polarization final observable. Karpenko and Becattini [20] showed that the difference between event-by-event simulations and an averaged initial condition to be small, albeit the source of Λ polarization in their work is different from ours.

Now we turn our attention to the jet thermalization. We consider a scenario of dijet creation inside the medium, where one jet will lose a negligible amount of energy and momentum while the other will be partially quenched, causing an asymmetry in jet emission. This

¹We attempted halving the grid spacing in x and y directions and our main results changed by only 1%, at the expense of a much greater computational effort.

Table 1: Input parameters for T_RENTo 3D.

Parameter	Value
Rapidity mean coefficient	0.0
Rapidity standard coefficient	2.9
Rapidity skewness coefficient	7.3
Skewness type	Relative skewness
Jacobian	0.75
Reduced thickness	0.007
Nucleon width	0.956 fm
Nucleon minimum distance	1.27 fm

is measured experimentally using the jet asymmetry observables A_J and x_J , defined as [4, 21, 22, 23]

$$x_J \equiv p_{T_2}/p_{T_1}, \quad (1)$$

$$A_J \equiv (E_{T_1} - E_{T_2})/(E_{T_2} + E_{T_1}). \quad (2)$$

The index “1” denote the trigger jet (the one that does not deposit energy and momentum in the medium) while the index “2” refers to the partially quenched jet.

From Eqs. (1) and (2), one can obtain the momentum (energy) of the quenched jet from the values of x_J (A_J) and the momentum (energy) of the trigger jet. Once E_{T_2} and p_{T_2} are determined, one may get the energy and momentum deposited in the medium as

$$\begin{aligned} p_{th} &= p_{T_1} - p_{T_2}, \\ E_{th} &= E_{T_1} - E_{T_2}. \end{aligned} \quad (3)$$

We will use the data from [4, Fig. 3] and [22, Fig. 8] to determine the values of p_{th} and E_{th} . These are the distribution of dN/dA_J and dN/dx_J for central Pb–Pb collisions at $\sqrt{s_{NN}} = 2.76$ TeV. The energy and momentum of the trigger jet in these measurements were $E_1 > 100$ GeV and $p_{T_1} = 89.5$ GeV/ c . For the values of A_J and x_J , we choose the ones that have the highest value of multiplicity, i.e. $A_J = 0.425$ and $x_J = 0.525$. This gives us $E_{th} = 59.6$ GeV and $p_{th} = 43$ GeV/ c . This implies that the situation studied in what follows corresponds to a dijet structure with a momentum of 89.5 GeV/ c for the unquenched jet and 59.5 GeV/ c for the partially quenched jet, noting that it is the latter that defines the direction in which lambda polarization will be studied.

The measurements that will be proposed later will be shown as a function of the difference between the azimuthal angle of the partially quenched jet and the emitted Λ . For simplicity, we choose the jet in the x -direction without loss of generality. With this choice, we may write the thermalized four-momentum as $p_{th}^\mu = (E_{th} \ p_{th} \ 0 \ 0)$ and build an

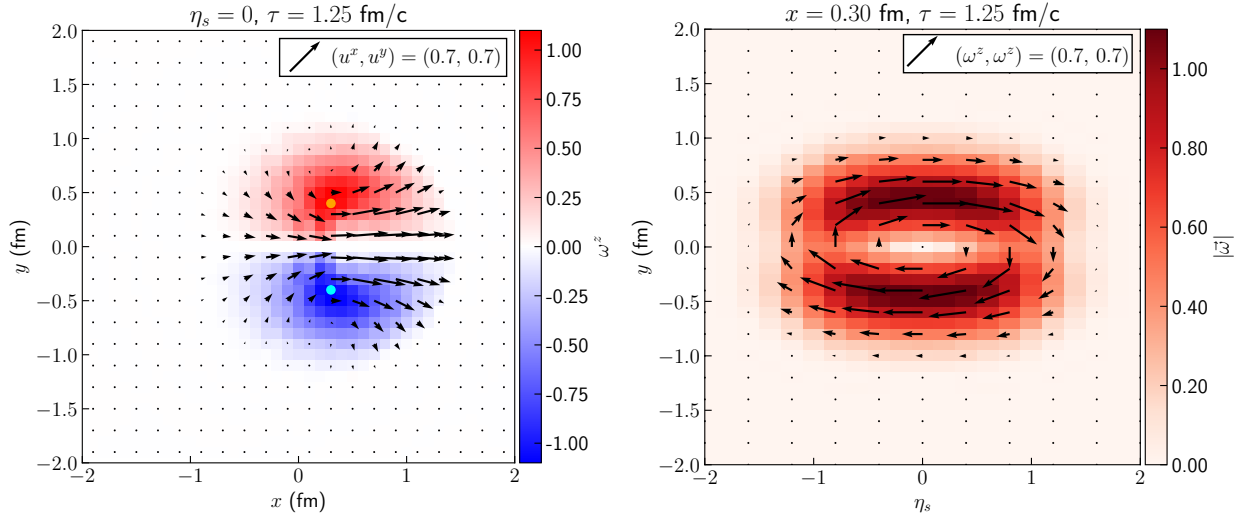


Figure 2: Vortex ring formed by the thermalized jet after $\Delta\tau = 1.00$ fm/c of hydrodynamic evolution. The jet deposited momentum in the \hat{x} direction, i.e. to the right in the left panel and away from the viewer in the right panel. In the left panel, it is shown a slice of the system at $\eta_s = 0$. The color map shows the z -component of vorticity vector defined in Eq. (8). The arrows shows the x and y components of the fluid's four-velocities. The dots marks the local maxima of $|\omega^z|$. On the right panel, the system is sliced along the position $x = 0.3$ fm. The color map shows $|\vec{\omega}|$ and the arrows shows the y and z components of the vorticity vector.

energy-momentum tensor $T^{\mu\nu}$ following

$$T^{\mu\nu} = \frac{1}{V} \frac{p_{th}^\mu p_{th}^\nu}{E_{th}}, \quad (4)$$

where V is the volume over which the energy and momentum is deposited. The volume is chosen to be an oblate spheroid centered on the origin of the system, with axis size equal to 0.5 fm in the x and y directions and ≈ 0.29 fm in the z -direction (which equates to $\eta_s \approx 1$ at $\tau = 0.25$ fm/c).

We apply the Landau matching procedure $T^{\mu\nu} u_\nu = \varepsilon u^\mu$ to solve for the local energy density and flow velocity from the energy-momentum tensor in Eq. (4)

$$\varepsilon = \frac{1}{V} \frac{E_{th}^2 - p_{th}^2}{E_{th}}, \quad (5)$$

$$u^x = \frac{p_{th}}{\sqrt{E_{th}^2 - p_{th}^2}}. \quad (6)$$

The remaining spatial components of u^μ are zero and u^τ is obtained by imposing the condition $u^\mu u_\mu = 1$. This procedure (energy-momentum tensor building and subsequent matching to a hydrodynamic-like energy-momentum tensor) was inspired by the procedure used for computing vorticity generated in the AMPT model in Ref. [24].

By inserting in Eqs. (5) and (6) the values for E_{th} and p_{th} obtained above, we obtain $\varepsilon V = 29$ GeV and

$v_x = 0.69 c$, where V is the volume over which the energy density will be deposited. In our simulations, we rounded these values to $\varepsilon V = 30$ GeV and $v_x = 0.7 c$. We verified that the injected energy-momentum generates on average 1% more final state particles per unit of pseudo-rapidity.

3. Fluid vorticity and polarization measurements

3.1. Jet induced fluid vorticity and Λ 's polarization

The described initial condition is evolved with 3D viscous hydrodynamics [25, 26, 27]. We use the lattice-QCD based equation of state from the HotQCD Collaboration [28] and start the evolution at $\tau = 0.25$ fm/c. The six independent components of the vorticity tensor are then saved over a hypersurface of $T = 151$ MeV. We then compute the mean spin of Λ following Eq. (2) of Ref. [15], which we reproduce below for completeness.

$$P^\mu(p) = -\frac{1}{8m} \varepsilon^{\mu\rho\sigma\tau} p_\tau \frac{\int d\Sigma_\lambda p^\lambda n_F (1 - n_F) \omega_{\rho\sigma}}{\int d\Sigma_\lambda p^\lambda n_F}, \quad (7)$$

$$n_F = \frac{1}{1 + \exp(\beta^\mu p_\mu - \mu Q/T)},$$

$$\omega^{\mu\nu} = -\frac{1}{2} (\partial^\mu \beta^\nu - \partial^\nu \beta^\mu) \quad \text{and} \quad \beta^\mu = \frac{u^\mu}{T}.$$

In our case, we do not consider baryon density and baryon currents and thus $\mu = 0$ MeV.

With the six components of the vorticity tensor $\omega^{\mu\nu}$ we calculate a vorticity vector ω^μ (inspired on the Pauli–Lubanski pseudovector), which will act as a proxy for the local spin polarization,

$$\omega^\mu \equiv \varepsilon^{\mu\nu\rho\epsilon} u_\nu \omega_{\rho\epsilon}. \quad (8)$$

In Figure 2, we show the spatial distributions of ω^z (along a slice of $\eta_s = 0$) and $|\vec{\omega}|$ (along a slice of $x = 0.3$ fm) at $\tau = 1.25$ fm/ c . The external energy-momentum from the jet induces a ring-shaped concentration of vorticity around the jet axis during the hydrodynamic evolution.

To verify the vortical structures in the fluid velocity field are mapped to the spin polarization of emitted Λ , we compare the averaged ω^z on the particlization hypersurface in the region $|\eta_s| < 0.5$ with the Λ 's P^z , averaged over the region $|y| < 0.5$ and $p_T < 3.0$ GeV/ c in Fig. 3. To obtain the azimuthal angle of each cell on the particlization hypersurface, we use the cell's four-velocity, i.e. $\varphi = \arctan(u^y/u^x)$. Since the fluid is expanding in a mostly radial way, the velocity angle φ is close to the spatial azimuthal angle of the cell. Figure 3 shows that the sign of Λ polarization correlates well with that of the fluid vorticity vector ω^μ in Eq. (8).

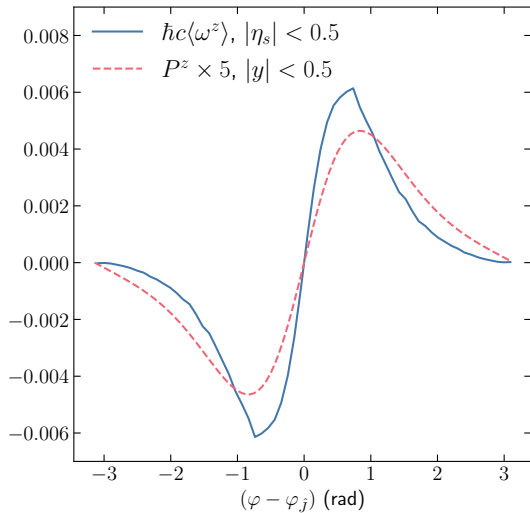


Figure 3: Comparison between the weighted average of the z -component of the vorticity vector (see Eq. 8) and the weighted average of the z -component of the Λ -polarization (see Eq. 7) at mid-rapidity.

Furthermore, we investigated the dependence of the z -component of the Λ -polarization (P^z) with transverse momentum and the angular distance (in the transverse plane) from the partially quenched jet, which we present

in Fig. 4 as a color map. The markers indicate the positions of the $|P^z|$'s maxima in each p_T -bin. The $|P^z|$'s maxima are closer to the jet axis at high p_T than those at low p_T bins.

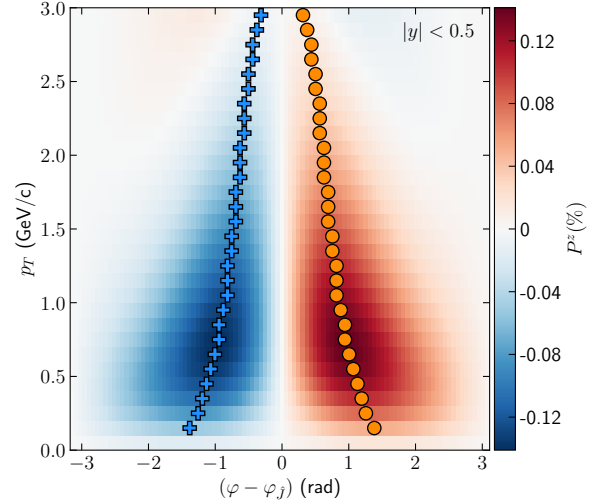


Figure 4: Distribution of the weighted average of the z -component of the polarization (P^z), using Λ -multiplicity as weight and as function of p_T and the angular distance in the transverse plane. The average considers only data in the range $|y| < 0.5$. The orange/blue dots marks the bins where $|P^z|$ is highest for that p_T bin.

3.2. The ring observable

We focused on the longitudinal component of polarization/vorticity for a jet that travels along the $+\hat{x}$ direction. Since the transverse components are anti-symmetric with respect to rapidity/spatial-rapidity (see Fig. 2, right panel), they will average to zero in the above calculations and we lose information about them. However, the formation of a vortex ring due to our choice of initial condition has similarities with the vortex rings present in p+A collisions which were studied in Ref. [29]. There we introduced the ring observable $\overline{\mathcal{R}}_\Lambda^{\hat{f}}$, which we replicate below for completeness

$$\overline{\mathcal{R}}_\Lambda^{\hat{f}} \equiv \left\langle \frac{\vec{P}_\Lambda \cdot (\hat{f} \times \vec{p}_\Lambda)}{|\hat{f} \times \vec{p}_\Lambda|} \right\rangle_{p_T, y}. \quad (9)$$

Here, $\hat{f} = \hat{J}$ is the axis direction of the jet², and $\langle \cdot \rangle_{p_T, y}$ denotes an weighted average over transverse momentum (in the range $0.5 \text{ GeV}/c < p_T < 3.0 \text{ GeV}/c$) and rapidity (in the range $|y| < 0.5$), using Λ multiplicity as

²on our calculation, $\hat{J} = \hat{x}$

weight. The use of $\overline{\mathcal{R}}_\Lambda^f$ will filter most contributions to the polarization which were not induced by the jet thermalization while allowing us to take into account effects in the direction besides \hat{z} . We will focus on $\overline{\mathcal{R}}_\Lambda^f$ from now on.

The use of thermal vorticity, as shown in Eq. 7, has been debated in the literature [30, 31, 32]. There are three other definitions of vorticity which are popularly employed. The “kinetic vorticity” consists of the replacement $\beta^\mu \rightarrow u^\mu$ and is appealing because it can be more intuitively interpreted. The “temperature vorticity” or “T-vorticity” relies on the replacement $\beta^\mu \rightarrow Tu^\mu$ and also allows vorticity generation by temperature gradients. Finally, there is the “spatially projected kinetic vorticity” which replaces the derivative ∂^μ by $\nabla^\mu = (g^{\mu\nu} - u^\mu u^\nu)\partial_\nu$. This has the effect of removing local acceleration terms from the kinetic vorticity. It also has a direct connection to the fluid vorticity in the non-relativistic limit. We show a comparison between the polarization results using these four different vorticity values in Fig. 5. The fact that polarization from kinetic, thermal, and temperature vorticities are essentially equal implies that in this case the vorticity is predominately generated by gradients in velocity, not in temperature. The higher value for the polarization from the spatially projected kinetic vorticity implies that local acceleration (caused mostly by the fluid expansion) has the effect of reducing the final Λ polarization.

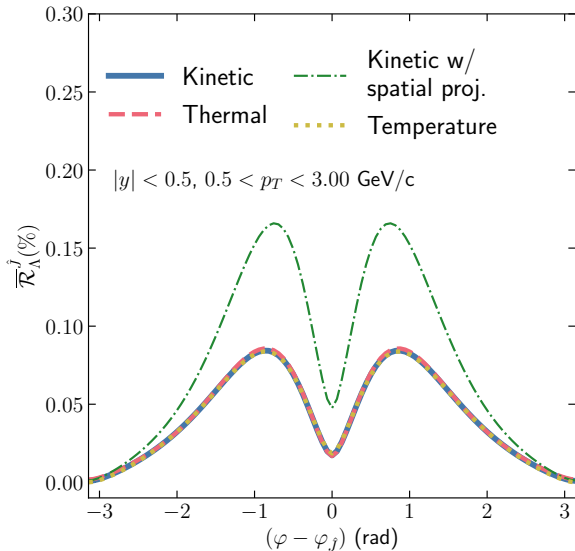


Figure 5: $\overline{\mathcal{R}}_\Lambda^f$ (see Eq. 9) computed from Λ -polarization calculations using four types of vorticity tensor.

We study the sensitivity of the ring observable $\overline{\mathcal{R}}_\Lambda^f$

on medium’s specific shear viscosity. In addition to $\eta/s = 0.08$, we perform calculations with $\eta/s = 0.00$, 0.01, 0.16 and 0.24. Figure 6 shows that the medium’s shear viscosity suppresses the ring observable $\overline{\mathcal{R}}_\Lambda^f$ ³. We observe a higher sensitivity of $\overline{\mathcal{R}}_\Lambda^f$ to small viscosity values $\eta/s < 0.08$ than $\eta/s > 0.08$. This trend is consistent with the vorticity ring being quenched by the medium, an effect which will be stronger for higher viscosity, but that eventually gets saturated. This is in contrast to elliptic flow, which has a more or less uniform dependence with viscosity [33].

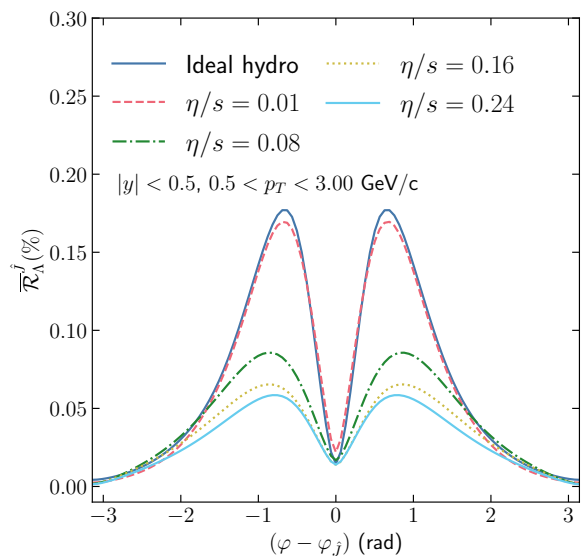


Figure 6: Distribution of $\overline{\mathcal{R}}_\Lambda^f$ (see Eq. 9) for different specific shear viscosities.

It is possible to argue that a jet which is quenched at the center of the system will not be accompanied by an unquenched jet. Instead, there would be a pair of quenched jets, inducing a pair back-to-back vortex rings. One could approximately treat the medium excitation from the two quenched jets as independent superposition (after rotating one of them by π rad). However, this would neglect the possibility of interactions between the two vortices during the hydrodynamic evolution. We investigate the possibility of a double-quenched jet by displacing the energy-momentum deposition to $x = 0.6$ fm. In the sequence, we add a second one at $x = -0.6$ fm with momentum in the opposite direction of the first. We compare the superposition scenario with the full simulation in Fig. 7. It is clear

³The angle where the signal is strong has a small dependence on viscosity as well.

to see that the superposition scenario has a polarization which is almost double the one where we evolve the two quenched jets, indicating the interaction between them during hydrodynamic evolution is crucial and has a self-canceling effect.

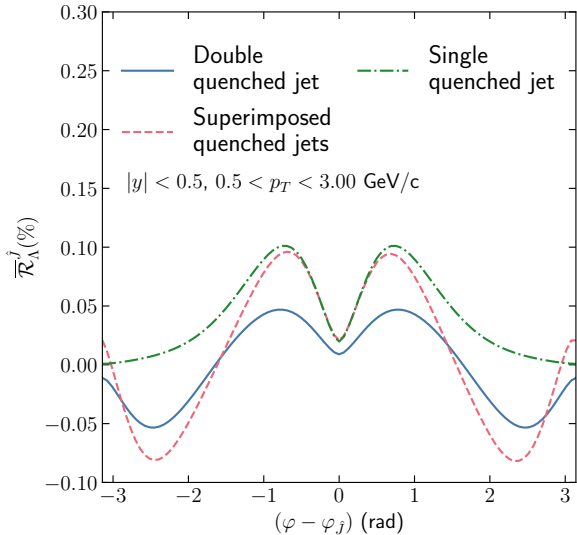


Figure 7: Comparison between the $\bar{\mathcal{R}}_\Lambda^f$ in a double-quenched jet scenario versus the single-quenched jet case. The blue curve shows the result from the simulation and the red one by superimposing two single-quenched jets (shown in green).

4. Conclusions

We modeled the thermalization of the energy-momentum from a hard parton as a “hot spot” which propagates inside fluid dynamic simulations. Such configuration of velocities will generate a vortex ring, which can be quantified by the vorticity of the fluid. The vorticity will lead to the emission of polarized hadrons on the particlization hypersurface as described in [30, 15].

To obtain the energy and momentum deposited in the medium by the jet thermalization, we assumed a jet with a transverse momentum of 89.5 GeV/c that would deposit approximately 40% of its energy in the medium, motivated by [4, Fig. 3] and [22, Fig. 8]. The polarized hadron emission would accompany a partially quenched jet, meaning that experimentally any analysis aiming to measure this effect would have to focus on an asymmetric jet pair, with the higher momentum jet having momentum of the order of 90 GeV/c and the lower momentum being of order 60 GeV/c. Other options, such

as using high-momentum trigger particles, will also be investigated in future work.

We computed the polarization of the Λ hyperon due to the vorticity caused by our model of jet thermalization. We showed that, for this specific case, the effects are dominated by velocity gradients and thus there is little difference in using thermal vorticity versus other definitions which are often suggested in the literature. We also showed that the strength of the signal is highly sensitive to the fluid’s shear viscosity.

The angular distribution of the ring observable $\bar{\mathcal{R}}_\Lambda^f$ in the transverse plane with respect to the quenched jet peaks in the range 0.5 rad to 1.0 rad, depending on transverse momentum. This position depends also on the shear viscosity as well, albeit in a more subtle way than the polarization amount. We also showed that the addition of a second quenched jet will not significantly affect the region where $\bar{\mathcal{R}}_\Lambda^f$ peaks. Instead, it will only dampen the overall magnitude in addition of an expected additional lobe in the opposite direction.

We point out that, despite the effect being of the order of only a few tenth of a percentiles, the proposed ring observable $\bar{\mathcal{R}}_\Lambda^f$ should be measurable by experiments, since it has the same of magnitude as reported per ALICE and STAR for the global Λ -polarization [16, 34]. We also inspected the typical maximum value found for $\bar{\mathcal{R}}_\Lambda^f$. We found that $\bar{\mathcal{R}}_\Lambda^f < 0.25\%$ always, peaking in the p_T range of $0.5 \text{ GeV}/c < p_T < 1.0 \text{ GeV}/c$.

We devote a future study to quantify the effects of event-by-event fluctuations in the fluid on $\bar{\mathcal{R}}_\Lambda^f$.

We note that the discussed jet induced polarization effect requires both color opacity and rapid thermalization. Thus, it is very likely present in AA and might disappear in pp and pA collisions (which may have rapid thermalization, but very small opacity). Since the reference is a high momentum trigger rather than a global quantity like the reaction plane, it should be possible for experiments to examine events with one Λ and one high momentum triggered hadron to verify this effect. If it turns out that indeed $\bar{\mathcal{R}}_\Lambda^f$ is non-zero for AA events, one could proceed to do more detailed model-data comparisons as a way to constrain viscosity and jet energy loss.

Acknowledgments

WMS, JGPB, DDC, JT and GT are supported by FAPESP projects 17/05685-2 (all), 19/05700-7 (WMS), 19/16293-3 (JPB) and 17/06508-7 (GT). MAL is supported by the U.S. Department of Energy grant DESC0020651 and acknowledges support of the Fulbright

Commission of Brazil. CS is supported by the U.S. Department of Energy under grant number DE-SC0013460 and the National Science Foundation under grant number PHY-2012922. GT acknowledges CNPQ bolsa de produtividade 301432/2017-1.

References

- [1] M. Gyulassy, M. Plumer, Jet Quenching in Dense Matter, *Phys. Lett. B* 243 (1990) 432–438. doi:10.1016/0370-2693(90)91409-5.
- [2] X.-N. Wang, M. Gyulassy, Gluon shadowing and jet quenching in A + A collisions at $s^{*}(1/2) = 200$ -GeV, *Phys. Rev. Lett.* 68 (1992) 1480–1483. doi:10.1103/PhysRevLett.68.1480.
- [3] U. A. Wiedemann, Jet Quenching in Heavy Ion Collisions, *Landolt-Bornstein* 23 (2010) 521. arXiv:0908.2306, doi:10.1007/978-3-642-01539-7_17.
- [4] G. Aad, et al., Observation of a Centrality-Dependent Dijet Asymmetry in Lead-Lead Collisions at $\sqrt{s_{NN}} = 2.77$ TeV with the ATLAS Detector at the LHC, *Phys. Rev. Lett.* 105 (2010) 252303. arXiv:1011.6182, doi:10.1103/PhysRevLett.105.252303.
- [5] S. Chatrchyan, et al., Observation and studies of jet quenching in PbPb collisions at nucleon-nucleon center-of-mass energy = 2.76 TeV, *Phys. Rev. C* 84 (2011) 024906. arXiv:1102.1957, doi:10.1103/PhysRevC.84.024906.
- [6] T. Schäfer, D. Teaney, Nearly Perfect Fluidity: From Cold Atomic Gases to Hot Quark Gluon Plasmas, *Rept. Prog. Phys.* 72 (2009) 126001. arXiv:0904.3107, doi:10.1088/0034-4885/72/12/126001.
- [7] K. Werner, I. Karpenko, M. Bleicher, T. Pierog, S. Porteboeuf-Houssais, Jets, Bulk Matter, and their Interaction in Heavy Ion Collisions at Several TeV, *Phys. Rev. C* 85 (2012) 064907. arXiv:1203.5704, doi:10.1103/PhysRevC.85.064907.
- [8] U. Heinz, R. Snellings, Collective flow and viscosity in relativistic heavy-ion collisions, *Ann. Rev. Nucl. Part. Sci.* 63 (2013) 123–151. arXiv:1301.2826, doi:10.1146/annurev-nucl-102212-170540.
- [9] C. Gale, S. Jeon, B. Schenke, Hydrodynamic Modeling of Heavy-Ion Collisions, *Int. J. Mod. Phys. A* 28 (2013) 1340011. arXiv:1301.5893, doi:10.1142/S0217751X13400113.
- [10] E. Shuryak, Strongly coupled quark-gluon plasma in heavy ion collisions, *Rev. Mod. Phys.* 89 (2017) 035001. arXiv:1412.8393, doi:10.1103/RevModPhys.89.035001.
- [11] C. Shen, L. Yan, Recent development of hydrodynamic modeling in heavy-ion collisions, *Nucl. Sci. Tech.* 31 (12) (2020) 122. arXiv:2010.12377, doi:10.1007/s41365-020-00829-z.
- [12] J.-P. Blaizot, Y. Mehtar-Tani, Jet Structure in Heavy Ion Collisions, *Int. J. Mod. Phys. E* 24 (11) (2015) 1530012. arXiv:1503.05958, doi:10.1142/S021830131530012X.
- [13] J. Takahashi, B. M. Tavares, W. L. Qian, R. Andrade, F. Grassi, Y. Hama, T. Kodama, N. Xu, Topology studies of hydrodynamics using two particle correlation analysis, *Phys. Rev. Lett.* 103 (2009) 242301. arXiv:0902.4870, doi:10.1103/PhysRevLett.103.242301.
- [14] B. Alver, G. Roland, Collision geometry fluctuations and triangular flow in heavy-ion collisions, *Phys. Rev. C* 81 (2010) 054905, [Erratum: *Phys.Rev.C* 82, 039903 (2010)]. arXiv:1003.0194, doi:10.1103/PhysRevC.82.039903.
- [15] F. Becattini, M. A. Lisa, Polarization and Vorticity in the Quark Gluon Plasma (3 2020). arXiv:2003.03640, doi:10.1146/annurev-nucl-021920-095245.
- [16] L. Adamczyk, et al., Global Λ hyperon polarization in nuclear collisions: evidence for the most vortical fluid, *Nature* 548 (2017) 62–65. arXiv:1701.06657, doi:10.1038/nature23004.
- [17] B. Betz, M. Gyulassy, G. Torrieri, Polarization probes of vorticity in heavy ion collisions, *Phys. Rev. C* 76 (2007) 044901. arXiv:0708.0035, doi:10.1103/PhysRevC.76.044901.
- [18] W. Ke, J. S. Moreland, J. E. Bernhard, S. A. Bass, Constraints on rapidity-dependent initial conditions from charged particle pseudorapidity densities and two-particle correlations, *Phys. Rev. C* 96 (4) (2017) 044912. arXiv:1610.08490, doi:10.1103/PhysRevC.96.044912.
- [19] J. E. Bernhard, Bayesian parameter estimation for relativistic heavy-ion collisions, Ph.D. thesis, Duke U. (4 2018). arXiv:1804.06469.
- [20] I. Karpenko, F. Becattini, Lambda polarization in heavy ion collisions: from RHIC BES to LHC energies, *Nucl. Phys. A* 982 (2019) 519–522. arXiv:1811.00322, doi:10.1016/j.nuclphysa.2018.10.067.
- [21] C. Young, B. Schenke, S. Jeon, C. Gale, Dijet asymmetry at the energies available at the CERN Large Hadron Collider, *Phys. Rev. C* 84 (2011) 024907. arXiv:1103.5769, doi:10.1103/PhysRevC.84.024907.
- [22] M. Aaboud, et al., Measurement of jet p_T correlations in Pb+Pb collisions at $\sqrt{s_{NN}} = 2.76$ TeV with the ATLAS detector, *Phys. Lett. B* 774 (2017) 379–402. arXiv:1706.09363, doi:10.1016/j.physletb.2017.09.078.
- [23] A. M. Sirunyan, et al., In-medium modification of dijets in PbPb collisions at $\sqrt{s_{NN}} = 5.02$ TeV (1 2021). arXiv:2101.04720.
- [24] H. Li, L.-G. Pang, Q. Wang, X.-L. Xia, Global Λ polarization in heavy-ion collisions from a transport model, *Phys. Rev. C* 96 (5) (2017) 054908. arXiv:1704.01507, doi:10.1103/PhysRevC.96.054908.
- [25] B. Schenke, S. Jeon, C. Gale, (3+1)D hydrodynamic simulation of relativistic heavy-ion collisions, *Phys. Rev. C* 82 (2010) 014903. arXiv:1004.1408, doi:10.1103/PhysRevC.82.014903.
- [26] B. Schenke, S. Jeon, C. Gale, Higher flow harmonics from (3+1)D event-by-event viscous hydrodynamics, *Phys. Rev. C* 85 (2012) 024901. arXiv:1109.6289, doi:10.1103/PhysRevC.85.024901.
- [27] J.-F. Paquet, C. Shen, G. S. Denicol, M. Luzum, B. Schenke, S. Jeon, C. Gale, Production of photons in relativistic heavy-ion collisions, *Phys. Rev. C* 93 (4) (2016) 044906. arXiv:1509.06738, doi:10.1103/PhysRevC.93.044906.
- [28] A. Bazavov, et al., Equation of state in (2+1)-flavor QCD, *Phys. Rev. D* 90 (2014) 094503. arXiv:1407.6387, doi:10.1103/PhysRevD.90.094503.
- [29] M. A. Lisa, J. a. G. P. Barbon, D. D. Chinellato, W. M. Serenone, C. Shen, J. Takahashi, G. Torrieri, Vortex rings from high energy central p+A collisions (1 2021). arXiv:2101.10872.
- [30] F. Becattini, G. Inghirami, V. Rolando, A. Beraudo, L. Del Zanna, A. De Pace, M. Nardi, G. Pagliara, V. Chandra, A study of vorticity formation in high energy nuclear collisions, *Eur. Phys. J. C* 75 (9) (2015) 406, [Erratum: *Eur.Phys.J.C* 78, 354 (2018)]. arXiv:1501.04468, doi:10.1140/epjc/s10052-015-3624-1.
- [31] Y. B. Ivanov, A. Soldatov, Vortex rings in fragmentation regions in heavy-ion collisions at $\sqrt{s_{NN}} = 39$ GeV, *Phys. Rev. C* 97 (4) (2018) 044915. arXiv:1803.01525, doi:10.1103/PhysRevC.97.044915.
- [32] I. Karpenko, Vorticity and Polarization in Heavy Ion Collisions: Hydrodynamic Models, 2021. arXiv:2101.04963.
- [33] P. Romatschke, U. Romatschke, Viscosity Information from Relativistic Nuclear Collisions: How Perfect is the Fluid Ob-

served at RHIC?, Phys. Rev. Lett. 99 (2007) 172301. arXiv:0706.1522, doi:10.1103/PhysRevLett.99.172301.

- [34] S. Acharya, et al., Global polarization of $\Lambda\bar{\Lambda}$ hyperons in Pb-Pb collisions at $\sqrt{s_{NN}} = 2.76$ and 5.02 TeV, Phys. Rev. C 101 (4) (2020) 044611. arXiv:1909.01281, doi:10.1103/PhysRevC.101.044611.